Photonic Crystal Light Collectors in Fish Retina Improve Vision in Turbid Water

Moritz Kreysing *et al.*

Science **336**, 1700 (2012);
DOI: 10.1126/science.1218072

function of this early pottery remains unknown. The Xianrendong assemblage contained a large number of fragmented bones, so the pottery could have been used in the extraction of marrow and grease (*24*, *25*). Other known uses of pottery in hunter-gatherer societies include food preparation and storage, as well as brewing alcoholic beverages, and could play a vital social role in feasting (*26*). Thus, the early invention of pottery may have played a key role in human demographic and social adaptations to climate change in East Asia, leading to sedentism, and eventually to the emergence of wild rice cultivation during the early Holocene (*17*, *27*).

References and Notes

1. P. B. Vandiver, O. Soffer, B. Klima, J. Svoboda, *Science* **246**, 1002 (1989).
2. P. Jordan, M. Zvelebil, Eds., *Ceramics Before Farming* (Left Coast Press, Walnut Creek, CA, 2009).
3. E. Boaretto *et al*., *Proc. Natl. Acad. Sci. U.S.A.* **106**, 9595 (2009).
4. Y. V. Kuzmin, P. A. Kosintsev, D. I. Razhev, G. W. Hodgins, *J. Hum. Evol.* **57**, 91 (2009).
5. C. T. Keally *et al*., *Radiocarbon* **48**, 345 (2004).
6. Jiangxi Provincial Cultural Relics Administration Committee, *Kao Gu Xue Bao* 1963.1, 1 (1963).
7. Jiangxi Provincial Museum, *Wen Wu* 1976.12, 23 (1976).
8. R. S. MacNeish, J. G. Libby, Eds., *Origins of Rice Agriculture: The Preliminary Report of the Sino-American Jiangxi (PRC) Project* (Publications in Anthropology no. 13, El Paso Centennial Museum, University of Texas at El Paso, El Paso, TX, 1995).
9. R. S. MacNeish *et al*., *Revised Second Annual Report of the Sino-American Jiangxi (PRC) Origin of Rice Project (SAJOR)* (Andover Foundation for Archaeological Research, Andover, MA, 1998).
10. L. Wang, Ed., *Human Pottery Making and Rice Cultivation: World-Class Archaeological Discoveries and Studies on the Xianrendong and Diaotonghuan Sites of Wannian County* (in Chinese) (Jiangxi Meishu Chubanshe, Nanchang, Jiangxi, People's Republic of China, 2010).
11. Z. Zhao, *Antiquity* **72**, 885 (1998).
12. M.-A. Courty, P. Goldberg, R. I. Macphail, *Soils and Micromorphology in Archaeology* (Cambridge Univ. Press, Cambridge, 1989).
13. P. Goldberg, R. I. Macphail, *Geoarchaeology* **18**, 571 (2003).
14. P. Goldberg, S. C. Sherwood, *Evol. Anthropol.* **15**, 20 (2006).
15. H. Brammer, *Geoderma* **6**, 5 (1971).
16. Detailed information for samples can be found in the supplementary materials, section S2.
17. Z. Zhao, *Curr. Anthropol.* **52**, S295 (2011).
18. D. Cohen, *Curr. Anthropol.* **52**, S273 (2011).
19. O. Bar-Yosef, *Curr. Anthropol.* **52**, S175 (2011).
20. E. Huang, J. Tian, S. Steinke, *Quat. Res.* **75**, 196 (2011).
21. J. Ni, G. Yu, S. P. Harrison, I. C. Prentice, *Palaeogeogr. Palaeoclimatol. Palaeoecol.* **289**, 44 (2010).
22. L. Barton, P. J. Brantingham, D. Ji, *Dev. Quat. Sci.* **9**, 105 (2007).
23. R. N. Carmody, G. S. Weintraub, R. W. Wrangham, *Proc. Natl. Acad. Sci. U.S.A.* **108**, 19199 (2011).
24. M. E. Prendergast, J. Yuan, O. Bar-Yosef, *J. Archaeol. Sci.* **36**, 1027 (2009).
25. J. Yuan, in *The Origins of Pottery and Agriculture*, Y. Yasuda, Ed. (Roli Books, New Delhi, India, 2002), pp. 157–166.
26. B. Hayden, *World Archaeol.* **34**, 458 (2003).
27. Z. Zhao, *Archaeol. Anthropol. Sci.* **2**, 99 (2010).

Acknowledgments: We thank the State Administration of Cultural Heritage of China for permission to carry out this project and the Jiangxi Provincial Institute of Cultural Relics and Archaeology for their support, in particular C. Fan and G. Zhou. W. Yan (Peking University) and B. Wang (Cultural Relics Bureau, Wannian, Jiangxi) provided assistance and information concerning the earlier excavations. We also thank S. Liu (Jiangxi Provincial Institute) for assistance. Detailed descriptions of the stratigraphy and the pottery fragments are in (*17*). We thank K. Liu and X. Ding for the atomic mass spectrometry (AMS) radiocarbon measurements. The American School of Prehistoric Research (Peabody Museum, Harvard University) supported the fieldwork and, in part, the preparation of the samples for microscopic analysis. P.G. is grateful to the NSF (grant no. 0917739) for partial support of this project. W.X., Z.C., and O.B.-Y. contributed to conceiving the project and organizing the fieldwork. P.G. and T.A. analyzed the micromorphology of the thin sections. W.X. and P.Y. conducted the dating of the new radiocarbon samples. W.X., O.B.-Y., P.G., Z.C., and D.C. prepared the paper. The authors declare no competing financial interests. Correspondence and requests for materials should be addressed to O.B.-Y. and X.W. (wuxh@pku.edu.cn).

Supplementary Materials

www.sciencemag.org/cgi/content/full/336/6089/1696/DC1
Materials and Methods
Supplementary Text
Figs. S1 to S24
Tables S1 to S4
References (*28*–*32*)

3 January 2012; accepted 1 May 2012
10.1126/science.1218643

Photonic Crystal Light Collectors in Fish Retina Improve Vision in Turbid Water

Moritz Kreysing,[1,2]* Roland Pusch,[3]* Dorothee Haverkate,[4]* Meik Landsberger,[3]* Jacob Engelmann,[3,5]* Janina Ruiter,[6] Carlos Mora-Ferrer,[7] Elke Ulbricht,[6,8] Jens Grosche,[6] Kristian Franze,[1,6,8] Stefan Streif,[9] Sarah Schumacher,[3] Felix Makarov,[10] Johannes Kacza,[11] Jochen Guck,[1,12] Hartwig Wolburg,[13] James K. Bowmaker,[14] Gerhard von der Emde,[3] Stefan Schuster,[4] Hans-Joachim Wagner,[15] Andreas Reichenbach,[6]† Mike Francke[1,6,16]

Despite their diversity, vertebrate retinae are specialized to maximize either photon catch or visual acuity. Here, we describe a functional type that is optimized for neither purpose. In the retina of the elephantnose fish (*Gnathonemus petersii*), cone photoreceptors are grouped together within reflecting, photonic crystal–lined cups acting as macroreceptors, but rod photoreceptors are positioned behind these reflectors. This unusual arrangement matches rod and cone sensitivity for detecting color-mixed stimuli, whereas the photoreceptor grouping renders the fish insensitive to spatial noise; together, this enables more reliable flight reactions in the fish's dim and turbid habitat as compared with fish lacking this retinal specialization.

Most vertebrate retinae have two types of photoreceptor cells: rods, capable of sensing one or a few photons, and cones, less light-sensitive by two orders of magnitude but wired to contrast- and color-sensitive neuronal circuits. Cones are "blind" in the dark whereas rods are saturated when cones are active, so typically there is only a small ("mesopic") range of light intensities at which both rods and cones contribute to vision. All presently known retinae are specialized for either cone-dominated high-acuity vision at daylight or rod-dominated maximum sensitivity in dim environments (*1*, *2*). Fitting neither description, the so-called "grouped retina" was already described 100 years ago as a puzzling retinal anomaly in some fish (*3*). In such retinae, many cones are grouped together inside large crystalline cups (*4*), which is incompatible with high spatial resolution (*5*). But the short rods

[1]Cavendish Laboratory, Department of Physics, University of Cambridge, Cambridge CB3 0HE, UK. [2]Systems Biophysics, Department of Physics, Ludwig-Maximilians University, D-80799 Munich, Germany. [3]Institute of Zoology, University of Bonn, D-53115 Bonn, Germany. [4]University of Bayreuth, Department of Animal Physiology, D-95440 Bayreuth, Germany. [5]Department of Biology, University of Bielefeld, D-33501 Bielefeld, Germany. [6]Paul-Flechsig-Institute for Brain Research, University of Leipzig, D-04109 Leipzig, Germany. [7]Institute of Zoology, Neurobiology, University Mainz, D-55099 Mainz, Germany. [8]Department of Physiology, Development and Neuroscience, University of Cambridge, Cambridge CB2 3EG, UK. [9]Institute for Automation Engineering, Systems Theory and Automatic Control Lab, Otto von Guericke University Magdeburg, D-39106 Magdeburg, Germany. [10]Pavlov Institute of Physiology, 199034 St. Petersburg, Russia. [11]Institute of Anatomy, Histology and Embryology, Faculty of Veterinary Medicine, University of Leipzig, D-04109 Leipzig, Germany. [12]Technische Universität Dresden, Biotechnology Center, D-01062 Dresden, Germany. [13]Institute of Pathology and Neuropathology, University of Tübingen, D-72076 Tübingen, Germany. [14]Institute of Ophthalmology, University College London, London EC1V 9EL, UK. [15]Institute of Anatomy, University of Tübingen, D-72074 Tübingen, Germany. [16]Translational Centre for Regenerative Medicine, University of Leipzig, D-04103 Leipzig, Germany.

*These authors contributed equally to this work.
†To whom correspondence should be addressed. E-mail: reia@medizin.uni-leipzig.de

are located behind these light-shielding cups, so this retina is not adapted for very dim light vision either (*1*).

We investigated the function and purpose of the grouped retina in the elephantnose fish (*Gnathonemus petersii*), using a variety of complementary techniques. (i) Light and electron microscopy (EM) of the grouped retina (Fig. 1) were used as a quantitative basis for (ii) electrodynamical simulations of light propagation inside the crystalline cups. (iii) Absorption spectra measurements of isolated cone and rod outer segments, as well as electroretinography on intact eyes, were applied to reveal the spectral sensitivities of the photoreceptors. (iv) Electrophysiological field potential recordings from the optic tectum served to characterize the stimulus processing. Finally, (v) several behavioral experiments tested how well the fish can detect predator-mimicking visual stimuli in comparison with goldfish (*Carassius auratus*) and pumpkinseed (*Lepomis gibbosus*), both with well-studied visually guided behavior based on high-acuity color vision.

Gnathonemus has a typical grouped retina (Fig. 1). Large bundles of inner and outer segments of photoreceptor cells are embedded in a sandglass-shaped scabbard formed by six adjacent giant retinal pigment epithelial (RPE) cells (Fig. 1, B to F, and movie S1). The shape of the scabbard and its contents undergo some changes between the light- and dark-adapted states (*6*); all our data were obtained under the daytime conditions (40 lx) found in the fish's dim habitats (*7*–*10*). In this light-adapted state, the upper part of the scabbard forms a reflective cup that is terminated by a constriction. This cup (Fig. 1, B and G) is directed toward the light and contains the light-insensitive inner segments of rods and cones. It was noteworthy that only the light-sensitive outer segments of cones (COSs) are located at its base, whereas the rod outer segments (ROSs) are embedded in the less regularly shaped part of the scabbard below the cup (at bottom in Fig. 1, B and G). Confocal microscopy and EM suggest that the inner surface of the cup acts as a mirror (Fig. 1D), formed by a reflecting multilayer of four layers of thin, evenly spaced rows of guanine-crystal lamellae (Fig. 1J, and fig. S2). The scabbard below the cup lacks a mirror surface but contains light-scattering, submicron-sized guanine crystallites and light-absorbing melanin granules (Fig. 1, G and I to K, and fig. S3B).

To rationalize this peculiar arrangement, we simulated the intensity distributions of the incident light inside and below the reflecting cups (Fig. 1H and fig. S4) using a finite-difference time-domain (FDTD) implementation of Maxwell's equations [see (*11*) and supplementary materials for details] with our morphological data and published data for the refractive indices of retinal neurons [$n = 1.36$; (*12*)] and of guanine [$n = 1.83$; (*13*)] as input parameters. These simulations show that (i) light is efficiently reflected from the walls of the cup, (ii) local intensity is increased by factors >5 at the cup bottom where the COSs are located (particularly, for deep-red wavelengths) (compare Fig. 2A and fig. S4), and (iii) only a small fraction of light reaches the rods. The wavelength dependence of the reflection has to be seen in light of the absorption spectra of the rods and the one type of cone identified morphologically. The measured absorption spectra of mechanically dissociated ROSs (Fig. 2B) and COSs (Fig. 2C) verified that there were single photopigments with maximum absorption at 536 nm ("green," rods) and at 615 nm ("red," all cones), respectively. Electroretinograms (ERGs), used to record electrical activity in the retina in response to visual stimuli, showed two corresponding maxima close to the absorption peaks of individual rods and cones (Fig. 2D). Note that the cone-driven peak of the ERG was slightly shifted toward longer wavelengths (Fig. 2D

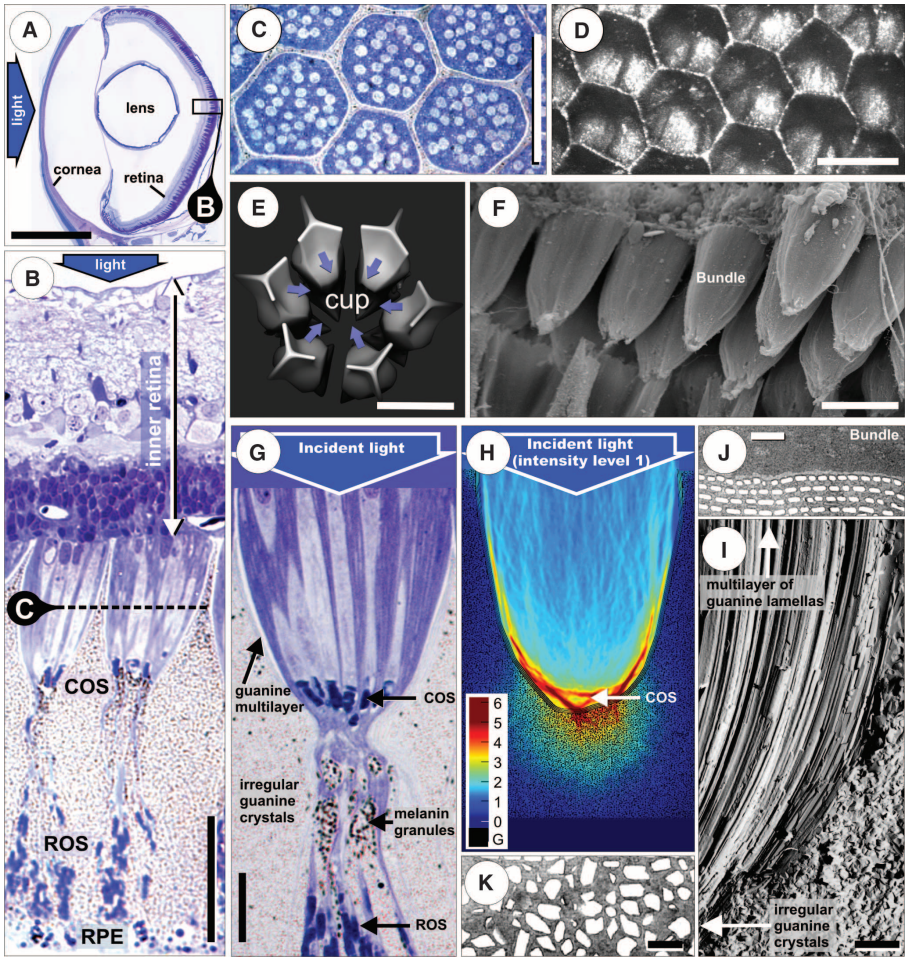

Fig. 1. The grouped retina of *Gnathonemus*. (**A**) Vertical section through an entire eye. (**B**) Radial semithin section at the region indicated in (A). The inner retina covers the crystalline cups, containing the COSs. ROSs are well below the cups and surrounded by RPE cells. (**C**) Transverse section through the cups at the level indicated in (B). The light blue circles are cone inner segments; rod inner segments are too thin to be visible. (**D**) Light reflection from the cups; top view onto intact retina using a confocal microscope in reflection mode. (**E**) Artistic rendering of six individual RPE cells, seen from top as in (D). The cells are here shifted away from each other, to demonstrate that the light-reflecting surfaces of six cells contribute to the formation of one cup (see also movie S1). (**F**) Scanning electron micrograph of several photoreceptor bundles—the filling of the cups. (**G**) Semithin section of a cup used as a model for the simulations with the COSs at its bottom and the ROSs far below, surrounded by RPE cells containing guanine crystals and melanin. (**H**) Simulation of the light intensity distribution in a cup for an incident plane wave of broad spectral range (525 to 725 nm). The COSs receive up to 500% of the incident light intensity, whereas the ROSs receive ≤20%. Color scale shows local gain; G stands for guanine (compare fig. S3). (**I**) Radial freeze-fracture electron micrograph of the guanine lamellae along the cup's inner surface. (**J** and **K**) Transmission electron micrographs of a transverse section through a cup wall, lined by rows of lamellae (J), and its bulk containing irregular crystals (K). Scale bars: 2 mm (A), 50 μm (B to F), 20 μm (G), 2 μm (I), 1 μm (J) and (K).

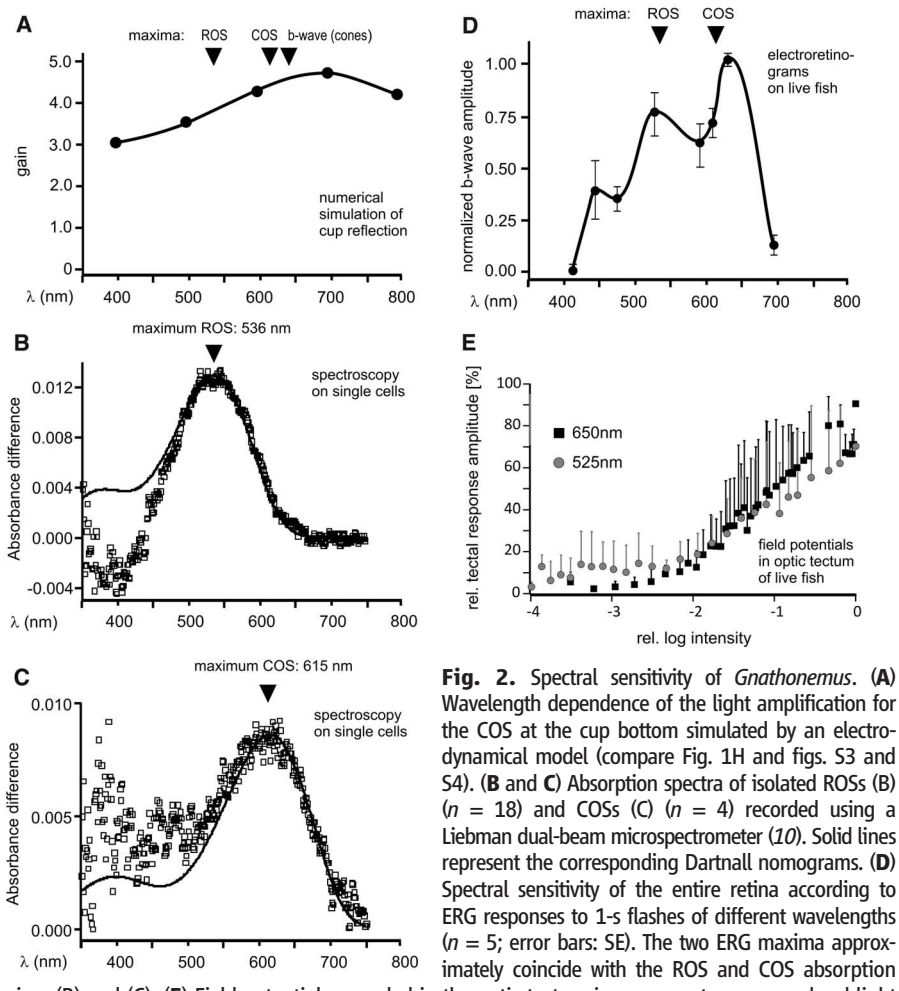

Fig. 2. Spectral sensitivity of *Gnathonemus*. (**A**) Wavelength dependence of the light amplification for the COS at the cup bottom simulated by an electrodynamical model (compare Fig. 1H and figs. S3 and S4). (**B** and **C**) Absorption spectra of isolated ROSs (B) (n = 18) and COSs (C) (n = 4) recorded using a Liebman dual-beam microspectrometer (*10*). Solid lines represent the corresponding Dartnall nomograms. (**D**) Spectral sensitivity of the entire retina according to ERG responses to 1-s flashes of different wavelengths (n = 5; error bars: SE). The two ERG maxima approximately coincide with the ROS and COS absorption maxima (B) and (C). (**E**) Field potentials recorded in the optic tectum in response to green and red light flashes of different intensities show that the tectal response of the fish is fully matched in sensitivity at both wavelengths.

versus 2C), in accordance with previously published data (*14*) that suggested a sensitivity of *Gnathonemus* to deep-red wavelengths, which is commensurate with the red-dominated turbid water it lives in (*8*, *14*, *15*) (fig. S1). This shift can be explained by the red-enhanced light reflection at the bottom of the photonic crystal cups (Fig. 2A and fig. S4).

The specific light distribution inside and below the crystalline cups holds the key for resolving the puzzle of the grouped retina, as it allows both cones and rods to be active simultaneously. The COSs—by themselves known to display a lower absolute light sensitivity than the ROSs (*16, 17*)—receive an elevated level of illumination, whereas the illumination of the ROSs is drastically reduced. The latter is advantageous because it prevents bleaching of rod photopigment and allows their use even under light-adapted conditions. Indeed, the ERGs invariably displayed a mixed rod-and-cone contribution to retinal electrical activity (Fig. 2D), whereas, in other animals, identical illumination conditions eliminate the rod responses from ERG recordings (*18*). By measuring visually evoked potentials in the optic tectum of *Gnathonemus* (n = 4), we confirmed that cone and rod photoreceptors were simultaneously activated over a nearly identical range of intermediate light intensities (Fig. 2E).

The behavioral consequences of this shared working range of rods and cones lie in a superior response to visual stimuli in the dim mesopic range of illumination compared with fish without a grouped retina. In fact, dim stimuli elicited a startle response in *Gnathonemus*, triggered by a rapidly expanding circle, much more reliably than in *Carassius,* whereas the control experiment in bright light showed no difference (Fig. 3A). The

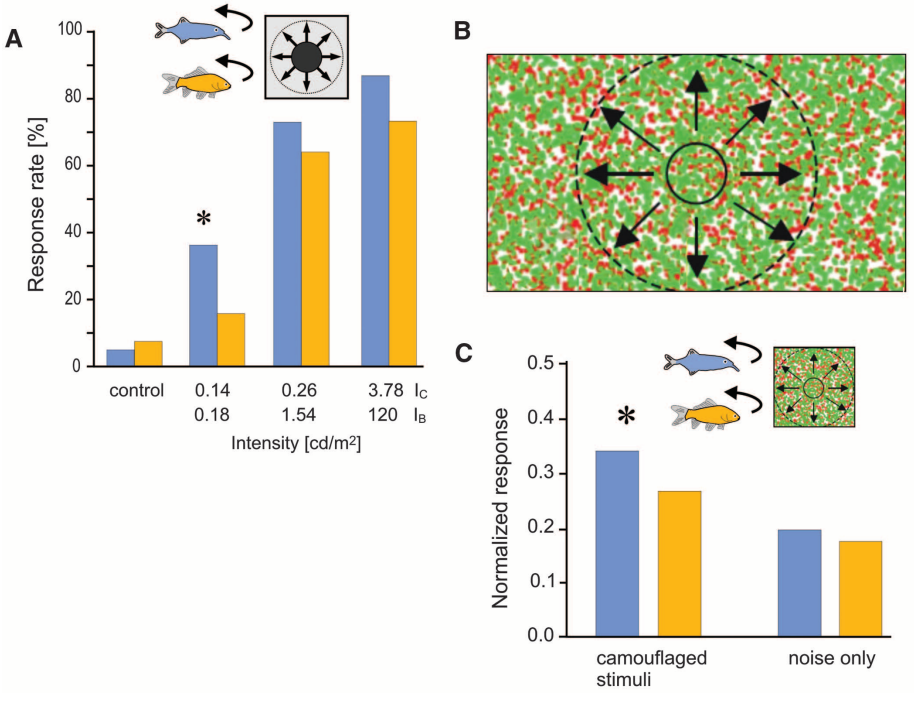

Fig. 3. *Gnathonemus* responds at low intensities and despite color camouflage. (**A**) Startle experiment with black circles expanding on a white background. The intensities of circles (I_C) and background (I_B) were varied. At low intensities, *Gnathonemus* (blue) performed better ($P < 0.05$) than *Carassius* (amber; n = 5 for both species). (**B**) Startle experiment with color-pooling task. The expanding circle was dynamically defined by the random exchange of red and green floating particles, with the particles inside the circle becoming stationary (compare movie S2). (**C**) *Gnathonemus* detected such color-camouflaged stimuli significantly better ($P < 0.05$) than *Carassius* (n = 5 for both species). The rate of false responses (right pair of columns) was not significantly different between species. Response percentages are relative to an expanding black circle that represents 1.0.

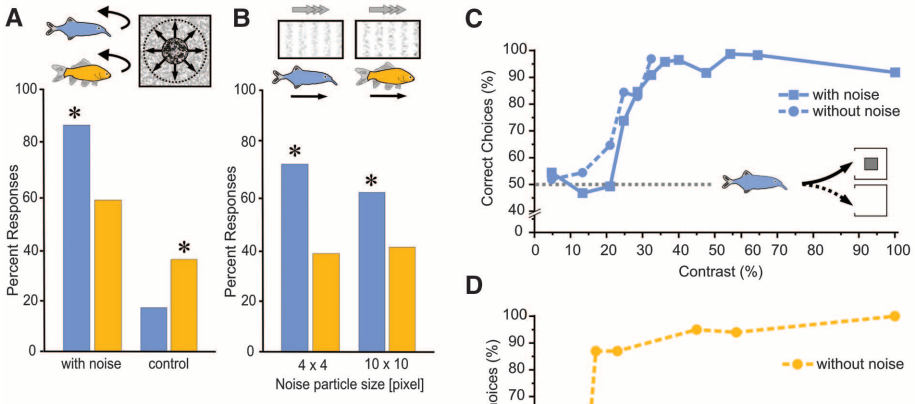

Fig. 4. *Gnathonemus* displays a high tolerance against spatial noise. (**A**) Startle experiment with an expanding circle disguised by dynamic gray noise particles (9000 particles). Flight responses declined in both species (percentage relative to no noise), but *Gnathonemus* (blue) was less affected than *Carassius* (amber; $P < 0.05$) and produced fewer false responses with noise only (control) ($P < 0.05$). (**B**) Percentage of optomotor responses to reversal of moving stripes relative to response rate without noise. When the stripes were obscured by dynamic white particles of varying size, *Gnathonemus* performed significantly better than *Carassius* ($P < 0.05$). (**C**) Contrast detection of *Gnathonemus* and (**D**) *Lepomis* with and without added dynamic noise particles. Fish were trained to approach a black square on a bright background; the contrast of the square was reduced stepwise. The performance of *Gnathonemus* decreased only slightly when noise particles were added (solid curve). Note that *Lepomis* refused to make any choices when images were overlaid by noise particles—even at 100% contrast.

color dependence of the startle response revealed a further remarkable advantage of *Gnathonemus*. Provided that *Gnathonemus* can add up signals from both cones (red) and rods (green) to generate responses to visual stimuli, such an addition (rather than a subtraction as required for color discrimination) should enable the detection of red-green color-camouflaged expanding stimuli, analogous to dichromatic human subjects and other dichromatic vertebrates (*19*, *20*). Indeed, *Gnathonemus* was better in detecting color-camouflaged objects, for example, when a rapidly expanding circle was only defined by randomly dynamic green and red dots (Fig. 3, B and C). Likewise, optomotor responses of *Gnathonemus*, assessed by its ability to follow the reversal of motion of a stripe pattern, could be elicited by green and red as well as white moving stripes (fig. S5A). This is in contrast to *Carassius*, whose optomotor response is selectively dependent on cone vision (*21*).

Additional behavioral advantages of *Gnathonemus* rest in the macroreceptor aspect of the grouped retina. On the one hand, behavioral tests confirmed that *Gnathonemus* detects only very large objects (4° and larger) (*5*, *6*, *22*), whereas objects of 3° visual field angle (corresponding to the sixfold diameter of the full moon in our eye) were not detected (fig. S5B). However, this apparent disadvantage was compensated for because *Gnathonemus* detected stimuli overlaid with noise in startle and optomotor tests better than *Carassius* and *Lepomis* did. When the expanding circle and the moving stripes were black on a white background, there was no statistical difference in the response between *Carassius* and *Gnathonemus*. But when a white or gray noise pattern was overlaid, *Gnathonemus* performed significantly better (Fig. 4, A and B). This improved noise tolerance was also obvious in the detection of large, stationary patterns, where *Gnathonemus* was only very little affected by the addition of small noise particles to the images, whereas *Lepomis* refused to accept noisy objects (Fig. 4, C and D). An obvious interpretation of these results is that the macroreceptors act as spatial low-pass filters before neuronal processing and render *Gnathonemus* incapable of resolving small-scale image information, whereas other fish with more acute vision get distracted by the image detail—an advantage *Gnathonemus* has when challenged with avoiding predators obscured by small debris and floating plant particles under poor lighting conditions.

Our results reveal that the photonic crystal cups in the grouped retina of *Gnathonemus* are effective, wavelength-sensitive light intensifiers that increase the sensitivity of cone photoreceptors in the red and match the dynamic ranges of rods and cones. This feature, together with the macroreceptor aspect of the grouped retina, enables these fish to perform better than species with conventional retinae, under experimental conditions mimicking the—visually challenging—habitat of *Gnathonemus*. We conclude that their grouped retina, as a unique type of retinal specialization, has emerged to provide the optical prerequisite to detect large, fast-moving predators as an adaptation to the survival demands of the fish's habitat. It might be expected that similar evolutionary advantages rationalize the grouped retina found in other species.

References and Notes

1. G. L. Walls, *The Vertebrate Eye and Its Adaptive Radiation* (Hafner Publ. Co, New York, 1963).
2. T. D. Lamb, S. P. Collin, E. N. Pugh Jr., *Nat. Rev. Neurosci.* **8**, 960 (2007).
3. A. Brauer, *Wiss. Ergebn. Tiefsee-Exped. "Valdivia" 1898-1899* **15**, 1 (1908).
4. N. A. Locket, *Proc. R. Soc. Lond. B Biol. Sci.* **178**, 161 (1971).
5. S. Schuster, S. Amtsfeld, *J. Exp. Biol.* **205**, 549 (2002).
6. M. Landsberger *et al.*, *J. Physiol. Paris* **102**, 291 (2008).
7. M. R. McEwan, *Acta Zool.* **19**, 427 (1938).
8. P. Moller, J. Serrier, P. Belbenoit, S. Push, *Behav. Ecol. Sociobiol.* **4**, 357 (1979).
9. P. Moller, *Electric Fishes: History and Behavior* (Chapman & Hall, London, 1995).
10. Materials and methods are available as supplementary materials on *Science* Online.
11. O. A. Oskooi *et al.*, *Comput. Phys. Commun.* **181**, 687 (2010).
12. K. Franze *et al.*, *Proc. Natl. Acad. Sci. U.S.A.* **104**, 8287 (2007).
13. M. C. J. Large, S. Wickham, J. Hayes, L. Poladian, *Physica B* **394**, 229 (2007).
14. S. Ciali, J. Gordon, P. Moller, *J. Fish Biol.* **50**, 1074 (1997).
15. R. D. Walmsley, M. Butty, H. Piepen, D. Grobler, *Hydrobiologia* **70**, 145 (1980).
16. F. S. Werblin, *Sci. Am.* **228**(1), 70 (1973).
17. R. A. Normann, F. S. Werblin, *J. Gen. Physiol.* **63**, 37 (1974).
18. M. W. Seeliger, A. Rilk, S. C. Neuhauss, *Doc. Ophthalmol.* **104**, 57 (2002).
19. M. J. Morgan, A. Adam, J. D. Mollon, *Proc. Biol. Sci.* **248**, 291 (1992).
20. S. Yokoyama, N. Takenaka, *Mol. Biol. Evol.* **22**, 968 (2005).
21. S. Schaerer, C. Neumeyer, *Vision Res.* **36**, 4025 (1996).
22. R. Rojas, P. Moller, *Brain Behav. Evol.* **59**, 211 (2002).

Acknowledgments: This work was financially supported by the Deutsche Forschungsgemeinschaft, the German Federal Ministry of Education and Research, and the Alexander-von-Humboldt Foundation. Help with freeze-fracturing by Ria Knittel is gratefully acknowledged. Numerical simulations were run on the Darwin Supercomputer, University of Cambridge. A.R., H.-J.W., S. Schuster, G.v.d.E., J. Guck, M.K., and M.F. developed the idea of the project, supervised the research, and wrote the manuscript; H.-J.W., J.E., F.M., E.U., R.P., J.R., H.W., J.K., and M.F. obtained morphological data; M.K. performed the electrodynamical simulations; J.B. measured the absorption spectra; K.F. measured light reflection of the eye; J. Grosche measured light reflection of the isolated retina and provided the 3D reconstructions of the RPE; M.L., D.H., and S. Schumacher obtained behavioral data; J.E. and R.P. performed tectum measurements; C.M.-F. and D.H. performed the electroretinogram; and S. Schuster designed and S. Streif developed the programs applied in the dynamic noise and color-pooling experiments.

Supplementary Materials

www.sciencemag.org/cgi/content/full/336/6089/1700/DC1
Materials and Methods
Figs. S1 to S5
References (*23*–*28*)
Movies S1 and S2

19 December 2011; accepted 14 May 2012
10.1126/science.1218072